Journal of Molecular Spectroscopy **197,** 1–11 (1999)
Article ID jmsp.1999.7885, available online at http://www.idealibrary.com on IDEAL®

Electronic Ground and Excited State Spectroscopy of C_6H and C_6D

H. Linnartz,* T. Motylewski,* O. Vaizert,* J. P. Maier,* A. J. Apponi,†,‡ M. C. McCarthy,†,‡ C. A. Gottlieb,‡ and P. Thaddeus†,‡

*Institute for Physical Chemistry, University of Basel, Klingelbergstrasse 80, CH 4056 Basel, Switzerland; †Harvard Smithsonian Center for Astrophysics, 60 Garden Street, Cambridge, Massachusetts 02138; and ‡Division of Engineering and Applied Sciences, Harvard University, Cambridge, Massachusetts 02138

E-mail: linnartz@ubaclu.unibas.ch

Received January 27, 1999; in revised form April 19, 1999

Rotational transitions in the $X^2\Pi$ ground state of C_6H and C_6D have been measured by Fourier transform microwave and millimeter-wave absorption spectroscopy. More than 150 rotational lines in the ground $^2\Pi_{3/2}$ and $^2\Pi_{1/2}$ ladders have been observed, allowing an accurate determination of the rotational, fine structure, lambda-doubling, and hyperfine coupling constants using a standard effective Hamiltonian for a molecule in an isolated $^2\Pi$ electronic state. The molecular ground state constants are used to characterize the rotationally resolved origin band of the $^2\Pi \leftarrow X^2\Pi$ electronic transition observed by cavity ring-down laser absorption spectroscopy in a pulsed supersonic slit-jet discharge source. From these data, spectroscopic constants for the excited electronic state are determined.

I. INTRODUCTION

Highly unsaturated carbon chains, the topic of many recent spectroscopic and astronomical studies (*1, 2*), are predicted to be key reactive intermediates in interstellar hydrocarbon chemistry. The carbon chains observed most extensively in space are the polar radicals CH through C_8H (*3, 4*). The hexatriynyl radical C_6H, the subject of this paper, has been observed by radio astronomers both in the cold, dense molecular cloud TMC-1 (*5, 6*) and in the molecular envelope of the carbon-rich star IRC+10216 (*6–8*). Large nonpolar pure carbon clusters (C_n) may also be present in the interstellar medium, but to date only C_3 and C_5 have been observed in circumstellar shells in the infrared (*9*).

Several homologous series of carbon chain radicals have been studied in the laboratory. Absorption spectra of mass-selected species in solid neon matrices have yielded a wealth of information, covering the spectral range from the UV to the IR (*10, 11*), but owing to solvation effects, the absorption bands exhibit a shift relative to the corresponding gas-phase spectra. The ground state spectroscopic constants for the free molecule have been obtained from microwave experiments for carbon chain radicals C_nH ($n \leq 14$), cyanopolyynes HC_nN ($n \leq 17$), and cumulenic carbenes H_2C_n ($n \leq 9$) (*1, 12, 13*), and from infrared spectra for neutral carbon chains C_n ($n \leq 13$) (*14*). Electronic transitions have been measured for the carbon chain anions C_n^- ($n \leq 11$) (*14–17*) by photodetachment spectroscopy and for the neutral carbon chain radicals $C_{2n}H$ by laser-induced fluorescence ($n = 2$) (*18*) and cavity ring-down absorption spectroscopy ($n = 3$–5) (*19, 20*). The latter show a strong $^2\Pi \leftarrow X^2\Pi$ transition which shifts by regular intervals to the red as the chain length increases.

Ab initio calculations on C_nH radicals provide estimates of the equilibrium structures, electric dipole moments, and energies of the excited electronic states (*21–23*). These predict that in C_6H, an excited $^2\Sigma$ electronic state lies very close in energy to the $^2\Pi$ ground state. The order of the $^2\Pi$ and $^2\Sigma$ states is reversed in the smaller members in the series and the ground state of C_2H and C_4H has $^2\Sigma$ symmetry. The electric dipole moments are calculated to be 5.9 D for the $^2\Pi$ and 1.2 D for the $^2\Sigma$ state of C_6H (*21*).

In this paper, a detailed spectroscopic study of the ground and electronically excited $^2\Pi$ state of C_6H and its deuterium-substituted isotope C_6D is presented. The microwave and millimeter-wave measurements reported here for C_6H are more accurate and extensive than the laboratory (*24*) and astronomical (*5, 7*) data in the literature, and as a result, the spectroscopic constants are more accurately determined than before. The electronic data yield spectroscopic constants for the excited $^2\Pi$ electronic state and provide an accurate measure of the band origin of the lowest ($^2\Pi_{3/2}$) spin component that is of relevance to astronomical observations. The measurements for C_6D allow for the first time an accurate spectroscopic characterization of this species.

II. EXPERIMENTS

A. Microwave and Millimeter Wave

The ground state rotational spectra of C_6H and C_6D were measured with a Fourier transform microwave (FTM) spec-

0022-2852/99 $30.00

trometer that operates between 5 and 26 GHz (*25*), and a millimeter-wave absorption spectrometer that operates in the range from 65 to 400 GHz (*26*). In the FTM experiment, C_6H and C_6D were produced in a supersonic molecular beam discharge source with a mixture of 0.25% diacetylene (HC_4H) or di-deutero diacetylene (DC_4D) in neon, under conditions similar to those that produce strong lines of $C_{10}H$, $C_{12}H$, $C_{13}H$, and $C_{14}H$ (*12*): a 110-μs long gas pulse, a backing pressure of 2 atm, and a 1100 V dc discharge in the throat of the supersonic expansion. Only the lowest spin component, $^2\Pi_{3/2}$, is thermally populated at the low ($\leq$3 K) rotational temperature of the molecular beam. Owing to the fairly long (2 ms) flight time of molecules through the Fabry–Perot cavity, very sharp lines (about 5 kHz FWHM) are observed. As a result, proton hyperfine structure (hfs) was easily resolved in C_6H and deuterium hfs was partially resolved in C_6D. Because the $^2\Pi_{3/2}$ spin component has a fairly large magnetic moment, care was taken to null out the Earth's magnetic field at the center of the Fabry–Perot cavity by means of three pairs of perpendicular Helmholtz coils. Adequate field cancellation was achieved for all but a few of the measurements; only for the lowest rotational transitions was the residual field large enough to broaden the lines beyond the intrinsic instrumental linewidth.

High rotational transitions of C_6H and C_6D were observed in both spin components between 70 and 220 GHz with the millimeter-wave absorption spectrometer. This is a standard absorption device which consists of a tunable source of millimeter-wave radiation, a 3-m long double-pass cell, and a liquid-He-cooled InSb bolometer. Fairly strong lines of C_6H and C_6D were produced in a 1000 V, 0.4 A dc glow discharge of HCCH (or DCCD) and argon in a 5:1 molar ratio.

B. Cavity Ring-Down

The $^2\Pi \leftarrow X^2\Pi$ electronic transition of C_6H and C_6D near 19 000 cm^{-1} (526 nm) were measured by cavity ring-down laser absorption spectroscopy. The instrumental details are described elsewhere (*27*). The molecules were produced in a pulsed supersonic plasma generated by discharging a mixture of 0.25% HCCH or DCCD in He in the throat of a 30 mm $\times$ 100-μm slit-jet nozzle (-600 to -1000 V, $\approx$80 mA) (*28*). This results in small Doppler linewidths, high molecular densities, a relatively long absorption path length, and effective adiabatic cooling. Rotational temperatures of less than 15 K are routinely obtained. The typical backing pressure is 10 atm, resulting in a pressure of less than 200 mTorr in the vacuum chamber at the 30 Hz repetition rate of the jet (1-ms pulse width). The cavity ring-down beam intersects the jet approximately 10 mm downstream from the throat of the nozzle. The light exiting the cavity is detected by a photo-multiplier and displayed on a fast oscilloscope. The ring-down events of 45 laser shots are averaged at each wavelength before the digitized data are downloaded to a workstation. Typical ring-down times of 30–50 μs are equivalent to an effective absorption path length through the supersonic expansion of roughly 1 km. The averaged ring-down time as a function of the laser frequency yields the spectral information. The spectra are calibrated and linearized via I_2 spectra that are recorded simultaneously in a small absorption cell. The experimental accuracy is limited by the laser bandwidth, which is about 0.035 cm^{-1} using an étalon in the dye laser cavity.

III. RESULTS AND DISCUSSION

$^2\Pi$ *Ground State*

Molecular constants for C_6H and C_6D were determined by numerically fitting a theoretical spectrum to the microwave and millimeter-wave measurements, using a standard effective Hamiltonian that includes hyperfine interactions for a linear molecule in an isolated $^2\Pi$ state (*29*, *30*). For C_6H, the data include 5 microwave and 25 millimeter-wave transitions up to $J = 78.5$ (Table 1 and 2); for C_6D, 4 microwave and 7 millimeter-wave transitions have been measured for the first time (Table 3 and 4). Lambda-doubling was resolved in all the observed transitions, but only the FTM data show evidence for hfs. A typical spectrum is shown in Fig. 1.

The centroids of the lambda-doublets are harmonically related for each rotational ladder except for a small shift owing to centrifugal distortion. All lines are fit to an rms of 35 kHz with only four parameters: the fine structure constant A'', rotational constant B'', centrifugal distortion constant D'', and spin–rotation constant γ''. When the hyperfine and lambda-doubling splittings are included, seven additional constants (two hyperfine and five lambda-doubling constants) are required to fit the individual lines to an rms uncertainty (39 kHz) that is about twice the measurement uncertainty (see Table 5). Small, systematic differences between the measured and calculated frequencies in Table 1 and 2 imply that the rotational levels in the ground vibrational state may be weakly perturbed by low-lying vibrationally excited states, interactions that are neglected in the Hamiltonian for an isolated $^2\Pi$ state. These interactions seem to be strongest at high J; when lines above 121 GHz are omitted, the rms (17 kHz) is nearly three times smaller.

The C_6H spectroscopic constants determined here are generally in good agreement with those previously derived from either the millimeter-wave laboratory data (*24*) or radio-astronomical observations (*5*). The sole exception is the hyperfine coupling constant $a + (b + c)/2$, which is smaller than previously thought because the off-diagonal term between the two spin components (proportional to the hyperfine coupling constant b) is not negligible (*31*). As a large number of additional C_6H lines have now been measured to high precision, one additional fourth-order lambda-doubling constant, p_H, was required to fit the laboratory data; if this constant is constrained to zero, the rms of the fit increases by nearly a factor of six.

As Table 5 shows, 10 spectroscopic constants are required to

TABLE 1
Measured Microwave Frequencies of C_6H

Transition $J' - J$	$F' - F$	Ω	e/f Λ Comp.[a]	Frequency (MHz)	o–c (kHz)
$3.5 \rightarrow 2.5$	$4 \rightarrow 3$	3/2	e	9703.508(10)	22
	$3 \rightarrow 2$		e	9703.600(10)	−13
	$4 \rightarrow 3$		f	9703.835(10)	13
	$3 \rightarrow 2$		f	9703.936(10)	−12
$4.5 \rightarrow 3.5$	$5 \rightarrow 4$	3/2	e	12475.888(5)	13
	$4 \rightarrow 3$		e	12475.973(5)	7
	$5 \rightarrow 4$		f	12476.448(5)	14
	$4 \rightarrow 3$		f	12476.534(5)	9
$5.5 \rightarrow 4.5$	$6 \rightarrow 5$	3/2	e	15248.247(5)	16
	$5 \rightarrow 4$		e	15248.322(5)	16
	$6 \rightarrow 5$		f	15249.084(5)	15
	$5 \rightarrow 4$		f	15249.158(5)	14
$6.5 \rightarrow 5.5$	$7 \rightarrow 6$	3/2	e	18020.574(5)	14
	$6 \rightarrow 5$		e	18020.644(5)	19
	$7 \rightarrow 6$		f	18021.752(5)	20
	$6 \rightarrow 5$		f	18021.818(5)	21
$7.5 \rightarrow 6.5$	$8 \rightarrow 7$	3/2	e	20792.872(5)	11
	$7 \rightarrow 6$		e	20792.945(5)	24
	$8 \rightarrow 7$		f	20794.444(5)	20
	$7 \rightarrow 6$		f	20794.512(5)	29

NOTE.— Uncertainties are 1σ experimental errors in the units of the last significant digits. The observed - calculated (o-c) are derived from the constants in Table 5.

[a]Designation of e and f levels is based on the assumption that the sign of the lambda-type doubling constant q is negative (see Table 5).

fit the C_6D lines to an rms of 16 kHz. Most of the constants are close to those expected from C_6H, including the deuterium hyperfine coupling constants $a + (b + c)/2$ and b, which scale approximately as $2\mu_D/\mu_H = 0.154$, where μ_H and μ_D are the nuclear magnetic moments for the proton and deuteron (*32*). Although the calculated spectra reproduce the observed C_6D lines much better than those of C_6H, this agreement may be misleading because the C_6D data set is smaller than that of C_6H and does not include lines with $J > 60.5$.

The relative sign of the lambda-doubling constants is determined from the normal isotopic species. Because the interval $2BJ$ between the rotational levels of the highest observed transitions is comparable to A'', it is more appropriate to use the individual lambda-doubling constants p and q for Hund's coupling case (b) rather than the case (a) combinations of $p + 2q$ and q. When the parities of the lambda doublets are chosen so that p and q are opposite in sign, the rms of the fit is two times larger (76 kHz) than when they have the same sign. When lines above 121 GHz are omitted, the rms of the two fits differ by a factor of 4 (68 versus 17 kHz). Although previous authors (*5*) assumed that q is positive, we take q to be negative by analogy with other C_nH chains (e.g., C_3H, C_5H, C_7H, etc.). For each of those radicals, q is always found to be negative on the assumption that the parity-dependent hyperfine constant d is positive.

Attempts to analyze a possible perturbation with a low-lying $^2\Sigma$ vibronic state have not been successful. In the closely related C_3H radical (*33*), the ground state rotational levels are perturbed by a Coriolis-type interaction with a $^2\Sigma$ vibronic state which is low lying because of a strong Renner–Teller interaction in the ν_4 CCH bend. In C_6H, fairly strong rotational lines from a low-lying $^2\Sigma$ vibronic state exhibit spin–rotation splittings that cannot be analyzed satisfactorily with a standard $^2\Sigma$ Hamiltonian. Nevertheless, no satisfactory fit using a Hamiltonian that explicitly accounts for a $^2\Pi$–$^2\Sigma$ interaction has been found for the ground state lines which is better than that obtained with the Hamiltonian for an isolated $^2\Pi$ state. Moreover, as a Coriolis-type interaction should be sensitive to the vibronic energy level pattern, and thus should differ for isotopic species, the close similarity of the C_6H and C_6D spectroscopic constants does not appear consistent with this type of perturbation (Table 5). An additional complication to the

TABLE 2
Measured Millimeter-wave Frequencies of C_6H

Transition $J' - J$	Ω	e/f Λ Comp.[a]	Frequency (MHz)	o–c (kHz)	Ω	e/f Λ Comp.[a]	Frequency (MHz)	o–c (kHz)
25.5 ← 24.5	3/2	e	70690.390(15)	9	1/2	f	71176.466(15)	−3
		f	70708.060(15)	62		e	71216.384(15)	48
26.5 ← 25.5	3/2	e	73462.273(15)	−3	1/2	f	73967.516(15)	−21
		f	73481.301(15)	46		e	74008.360(15)	37
27.5 ← 26.5	3/2	e	76234.155(15)	1	1/2	f	76758.492(15)	−8
		f	76254.587(15)	46		e	76800.308(15)	41
28.5 ← 27.5	3/2	e	79006.011(15)	−5	1/2	f	79549.383(15)	−6
		f	79027.898(15)	44		e	79592.201(15)	34
29.5 ← 28.5	3/2	e	81777.856(15)	−7	1/2	f	82340.201(15)	−1
		f	81801.237(15)	42		e	82384.050(15)	28
30.5 ← 29.5	3/2	e	84549.688(15)	−5	1/2	f	85130.946(15)	10
		f	84574.600(15)	36		e	85175.846(15)	18
31.5 ← 30.5	3/2	e	87321.504(15)	−5	1/2	f	87921.593(15)	2
		f	87347.994(15)	35		e	87967.595(15)	12
32.5 ← 31.5	3/2	e	90093.295(15)	−15	1/2	f	90712.181(15)	16
		f	90121.407(15)	27		e	90759.297(15)	12
33.5 ← 32.5	3/2	e	92865.078(15)	−18	1/2	f	93502.677(15)	21
		f	92894.848(15)	20		e	93550.939(15)	7
34.5 ← 33.5	3/2	e	95636.852(15)	−17	1/2	f	96293.084(15)	22
		f	95668.308(15)	8		e	96342.532(15)	10
35.5 ← 34.5	3/2	e	98408.607(15)	−21	1/2	f	99083.408(15)	26
		f	98441.812(15)	14		e	99134.050(15)	−3
36.5 ← 35.5	3/2	e	101180.347(15)	−27	1/2	f	101873.640(15)	24
		f	101215.315(15)	−4		e	101925.512(15)	−10
37.5 ← 36.5	3/2	e	103952.075(15)	−32	1/2	f	104663.787(15)	27
		f	103988.861(15)	−4		e	104716.909915)	−19
38.5 ← 37.5	3/2	e	106723.796(15)	−32	1/2	f	107453.845(15)	31
		f	106762.421(15)	−12		e	107508.254(15)	−13
39.5 ← 38.5	3/2	e	109495.493(15)	−43	1/2	f	110243.798(15)	22
		f	109535.996(15)	−27		e	110299.519(15)	−20
40.5 ← 39.5	3/2	e	112267.200(15)	−33	1/2	f	113003.681(15)	37
		f	112309.594(15)	−41		e	113090.722(15)	−19
41.5 ← 40.5	3/2	e	115038.882(15)	−35	1/2	f	115823.453(15)	35
		f	115083.223(15)	−45		e	115881.842(15)	−29
42.5 ← 41.5	3/2	e	117810.539(15)	−52	1/2	f	118613.134(15)	37
		f	117856.886(15)	−35		e	118672.897(15)	−30
43.5 ← 42.5	3/2	e	120582.196(15)	−57				
		f	120630.543(15)	−51				
60.5 ← 59.5	3/2	e	167698.922(15)	6	1/2	f	168809.442(15)	−58
		f	167784.918(15)	−150		e	168897.082(15)	−43
62.5 ← 61.5	3/2	e	173241.877(15)	5	1/2	f	174384.556(15)	−74
		f	173332.621(15)	−163		e	174475.572(15)	−28
64.5 ← 63.5					1/2	f	179959.198(15)	−82
67.5 ← 66.5	3/2	e	187099.101(15)	22	1/2	f	188320.242(15)	−96
						e	188419.784(15)	−26
77.5 ← 76.5	3/2	e	214812.643(15)	25	1/2	f	216182.376(15)	32
		f	214939.775(15)	56		e	216299.186(15)	34
78.5 ← 77.5	3/2	e	217583.914(15)	16	1/2	f	218967.931(15)	101
		f	217713.497(15)	108		e	219086.404(15)	22

NOTE. Uncertainties are 1σ experimental errors in the units of the last significant digits. The observed-calculated (o-c) are derived from the constants in Table 5.

[a] Designation of e and f levels is based on the assumption that the sign of the lambda-type doubling constant q is negative (see Table 5).

TABLE 3
Measured Microwave Frequencies of C_6D

Transition $J' - J$	$F' - F$	Ω	e/f Λ Comp.[a]	Frequency (MHz)	o–c (kHz)
$6.5 \rightarrow 5.5$	$7.5 \rightarrow 6.5$	3/2	e	17202.424(5)	0
	$6.5 \rightarrow 5.5$		e	17202.443(5)	4
	$5.5 \rightarrow 4.5$		e	17202.452(5)	−1
	$7.5 \rightarrow 6.5$		f	17203.485(5)	−1
	$6.5 \rightarrow 5.5$		f	17203.503(5)	2
	$5.5 \rightarrow 4.5$		f	17203.511(5)	−4
$7.5 \rightarrow 6.5$	$8.5 \rightarrow 7.5$	3/2	e	19848.862(5)	−1
	$7.5 \rightarrow 6.5$		e	19848.878(5)	1
	$6.5 \rightarrow 5.5$		e	19848.889(5)	−1
	$8.5 \rightarrow 7.5$		f	19850.277(5)	−1
	$7.5 \rightarrow 6.5$		f	19850.292(5)	0
	$6.5 \rightarrow 5.5$		f	19850.304(5)	−1
$8.5 \rightarrow 7.5$	$9.5 \rightarrow 8.5$	3/2	e	22495.278(2)	0
	$8.5 \rightarrow 7.5$		e	22495.293(2)	2
	$7.5 \rightarrow 6.5$		e	22495.303(2)	0
	$9.5 \rightarrow 8.5$		f	22497.096(2)	0
	$8.5 \rightarrow 7.5$		f	22497.110(2)	1
	$7.5 \rightarrow 6.5$		f	22497.120(2)	−1
$9.5 \rightarrow 8.5$	$10.5 \rightarrow 9.5$	3/2	e	25141.668(2)	−1
	$9.5 \rightarrow 8.5$		e	25141.682(2)	0
	$8.5 \rightarrow 7.5$		e	25141.695(2)	1
	$10.5 \rightarrow 9.5$		f	25143.940(2)	0
	$9.5 \rightarrow 8.5$		f	25143.953(2)	1
	$8.5 \rightarrow 7.5$		f	25143.964(2)	0

NOTE.— Uncertainties are 1σ experimental errors in the units of the last significant digits. The observed - calculated (o-c) are derived from the constants in Table 5.

[a]Designation of e and f levels is based on the assumption that the sign of the lambda-type doubling constant q is negative (see Table 5).

ground state spectrum may be caused by interactions with the lowest $^2\Sigma$ electronic state. The large observed spin–rotation constant γ'' and small spin–orbit constant A'' compared with those of other C_nH radicals, provide indirect evidence that such an interaction may occur. Detection of rotational lines from other vibronic states and additional theoretical calculations of the low-lying energy level structure are needed before a more complete analysis of the C_6H spectrum in the ground electronic state can be undertaken.

$^2\Pi \leftarrow X^2\Pi$ *Electronic Transition*

The initial observation of the origin band of the $^2\Pi \leftarrow X^2\Pi$ electronic transition of C_6H was in a hollow cathode discharge cell (*19*). These gas-phase data were unresolved, prohibiting a rotational analysis, and owing to the temperature in the cell, >200 K, an unambiguous assignment of the two spin–orbit components was not possible. In the present experiment the low rotational temperature (typically less than 15 K) and the small Doppler broadening in the 2-dimensional jet allow straightforward spin–orbit and rotational assignments. In Fig. 2 the rotationally resolved $\Omega = \frac{3}{2}$ and $\frac{1}{2}$ spin–orbit components of the $^2\Pi \leftarrow X^2\Pi$ origin band of C_6H are shown. The relative intensity of the spin–orbit components is determined by the temperature in the jet and the size of the spin–orbit splitting in the ground state. Using the A'' values derived for C_6H and C_6D (Table 5), an averaged spin–orbit temperature of ≈15 K is calculated, which agrees well with the rotational temperature derived from the rotational profile. As the ground state is inverted, this also indicates that the stronger band, i.e., the one at lower energy, belongs to the $^2\Pi_{3/2} \leftarrow X^2\Pi_{3/2}$ system and thus $|A'| > |A''|$.

TABLE 4
Measured Millimeter-wave Frequencies of C_6D

Transition $J' - J$	Ω	e/f Λ Comp.[a]	Frequency (MHz)	o–c (kHz)	Ω	e/f Λ Comp.[a]	Frequency (MHz)	o–c (kHz)
53.5 ← 52.5	3/2	e	141565.117(15)	−68	1/2	f	142484.522(15)	−6
		f	141628.682(15)	−31		e	142554.673(15)	16
54.5 ← 53.5	3/2	e	144210.839(15)	−33	1/2	f	145145.990(15)	6
		f	144276.453(15)	−26		e	145217.542(15)	10
55.5 ← 54.5	3/2	e	146856.550(15)	1	1/2	f	147807.355(15)	9
		f	146924.233(15)	−19		e	147880.310(15)	−8
56.5 ← 55.5	3/2	e	149502.225(15)	10	1/2	f	150468.618(15)	6
		f	149572.031(15)	2		e	150542.993(15)	−20
57.5 ← 56.5	3/2	e	152147.890(15)	19	1/2	f	153129.787(15)	5
		f	152219.815(15)	3		e	153205.605(15)	−9
58.5 ← 57.5	3/2	e	154793.536(15)	20	1/2	f	155790.833(15)	−23
		f	154867.614(15)	17		e	155868.123(15)	2
59.5 ← 58.5	3/2	e	157439.178(15)	28	1/2	f	158451.835(15)	4
		f	157515.424(15)	39		e	158530.540(15)	10

NOTE.— Uncertainties are 1σ experimental errors in the units of the last significant digits. The observed - calculated (o-c) frequencies are derived from the constants in Table 5.

[a]Designation of e and f levels is based on the assumption that the sign of the lambda-type doubling constant q is negative (see Table 5).

The rotational assignment confirms this conclusion; the lower ($\Omega = \frac{3}{2}$) component has a band gap of $\approx 10B$, the other component $\approx 6B$ (Fig. 2). In addition, there is a pronounced difference in intensity of the Q branches; whereas the Q branch for $\Omega = \frac{3}{2}$ is clearly visible at 18 985.4 cm^{-1}, it is hard to observe it at 18 994.1 cm^{-1} for $\Omega = \frac{1}{2}$ (19 036.8 and 19 045.7

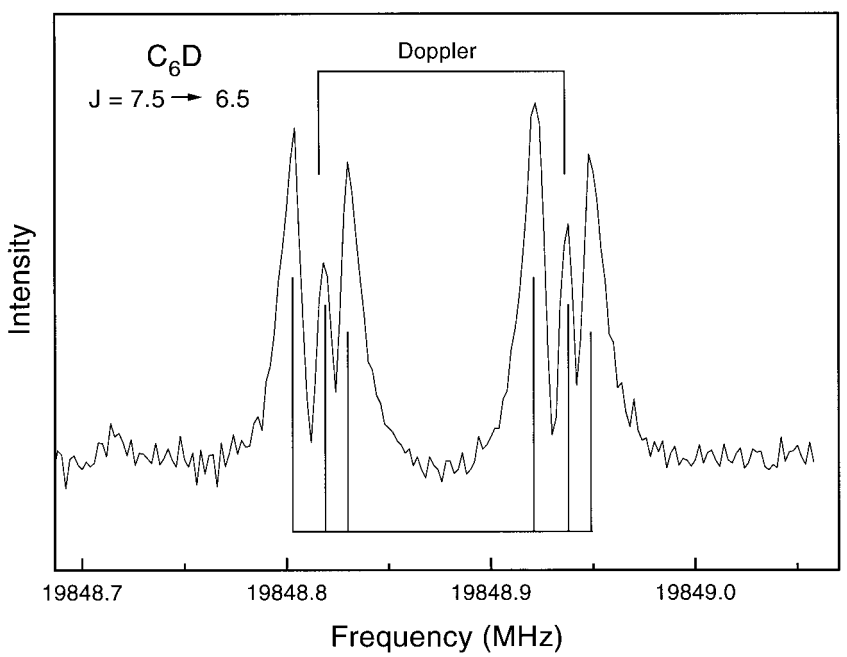

FIG. 1. Sample line of C_6D ($\Omega = \frac{3}{2}$, $J = 7.5 \rightarrow 6.5$, e) obtained in an integration time of 5 min, showing well-resolved deuterium hyperfine structure. The double-peaked line profiles are instrumental in origin, the Doppler splitting that results when the Mach 2 axial molecular beam interacts with the standing wave in the confocal Fabry–Perot cavity of the spectrometer.

TABLE 5
Spectroscopic Constants of Ground State C_6H and C_6D

Constant[a]	C_6H	C_6D
A_{eff}	−450961(46)	−453514(48)
	(−15.04 cm^{-1})	(−15.13 cm^{-1})
B	1391.18612(3)	1327.85374(5)
	(0.046404974(1) cm^{-1})	(0.044292427(2) cm^{-1})
$D \times 10^6$	40.49(1)	36.04(1)
γ	−213.5(1)	−226.1(1)
p	−24.62(1)	−21.32(10)
$p_D \times 10^3$	2.738(5)	1.97(1)
$p_H \times 10^9$	−70.1(5)	...
q	−1.4572(2)[a]	−1.3741(6)[a]
$q_D \times 10^6$	15.70(3)	15.2(1)
$a + (b + c)/2$	0.60(67)	0.12(26)
b	−13.0(15)	−3.20(72)

NOTE.— Units are MHz. The 1σ uncertainties are in the units of the last significant digits.

[a]Sign assumed to be negative.

cm^{-1}, respectively, for C_6D). This is as expected for the low temperature in the experiment and a linestrength S_{JJ} for the Q branch that is given by $S_{JJ} = \Omega^2(2J + 1)/(J(J + 1))$.

The line positions and assignment for the C_6H and C_6D transitions are given in Tables 6 and 7, respectively. No splittings due to lambda-doubling have been observed. Because

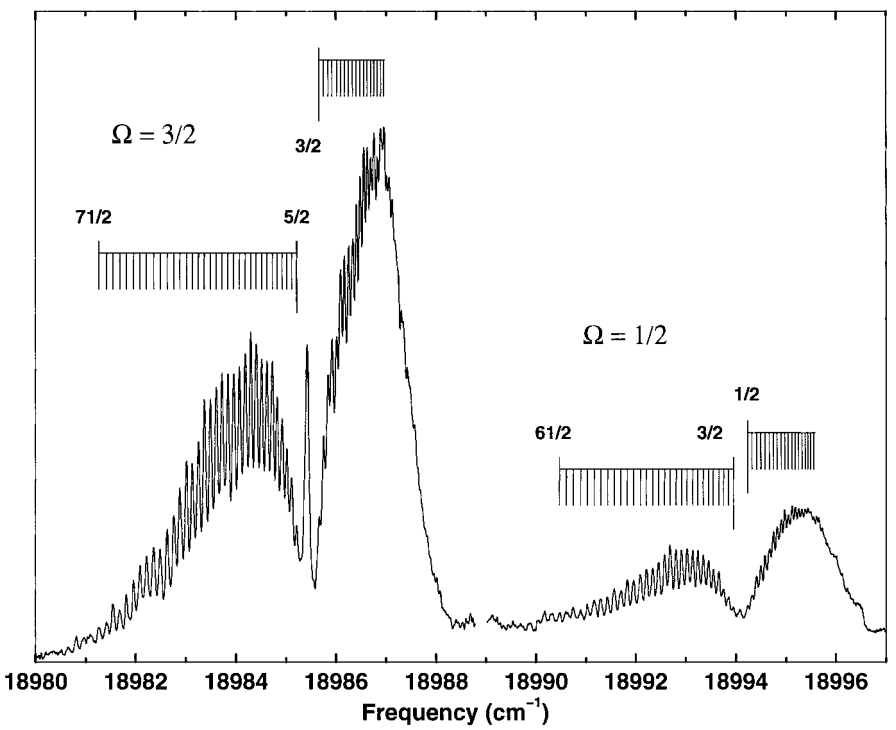

FIG. 2. The two spin–orbit components in the origin band of the $^2\Pi \leftarrow X^2\Pi$ electronic transition of C_6H measured by cavity ring-down spectroscopy in a supersonic slit jet plasma. The rotational temperature is ≈15 K.

TABLE 6
Measured Rotational Frequencies of the 0_0^0 $^2\Pi \leftarrow X^2\Pi$ Transition of C_6H

Transition J	ν (cm^{-1})	o–c ($10^{-3}cm^{-1}$)	ν (cm^{-1})	o–c ($10^{-3}cm^{-1}$)
$\Omega = 3/2$	P-branch		R-branch	
1.5			18985.660	−12
2.5	18985.210	−3	18985.749	−10
3.5	18985.110	−6	18985.842	−2
4.5	18985.014	−4	18985.919	−10
5.5	18984.919	−1	18986.011	0
6.5	18984.819	1	18986.092	−1
7.5	18984.726	9	18986.166	−6
8.5	18984.618	5	18986.251	0
9.5	18984.510	2	18986.333	6
10.5	18984.404	3	18986.403	0
11.5	18984.296	3	18986.478	2
12.5	18984.186	2	18986.554	5
13.5	18984.068	−4	18986.622	2
14.5	18983.959	−1	18986.691	1
15.5	18983.841	−4	18986.757	0
16.5	18983.720	−10	18986.823	−1
17.5	18983.607	−6	18986.890	1
18.5	18983.489	−5	18986.957	5
19.5	18983.371	−3		
20.5	18983.255	2		
21.5	18983.128	−2		
22.5	18983.014	8		
23.5	18982.881	2		
24.5	18982.762	9		
25.5	18982.629	6		
26.5	18982.487	−6		
27.5	18982.359	−2		
28.5	18982.215	−12		
29.5	18982.085	−7		
30.5	18981.955	0		
31.5	18981.808	−8		
32.5	18981.682	4		
33.5	18981.545	8		

NOTE. The observed-calculated (o-c) are derived from the constants in Tables 5 and 8.

both *P*- and *R*-branch transitions are available, combination differences have been calculated, yielding values for the ground state rotational levels. These agree well within the experimental uncertainty with the values calculated from the microwave constants listed in Table 5. The line positions are fit with an effective Hamiltonian using the ground state parameters given in Table 5, with the band origin (T_0), effective rotational constant (B'), and spin–orbit interaction coefficient (A') of the upper electronic state as adjustable parameters. Inclusion of the centrifugal distortion constant does not appreciably improve the fit and yields a rather inaccurate value for D'. Therefore D' was fixed to the ground state value, as was done for the spin–rotation and lambda-doubling constants. The two spin–orbit components were fit simultaneously, yielding

TABLE 6—*Continued*

Transition J	ν (cm^{-1})	o–c ($10^{-3}cm^{-1}$)	ν (cm^{-1})	o–c ($10^{-3}cm^{-1}$)
34.5	18981.417	22		
35.5	18981.267	17		
$\Omega = 1/2$	P-branch		R-branch	
0.5			18994.236	9
1.5	18993.948	−2	18994.318	3
2.5	18993.848	−6	18994.408	5
3.5	18993.752	−5	18994.495	7
4.5	18993.658	1	18994.575	4
5.5	18993.549	−7	18994.667	13
6.5	18993.451	−2	18994.747	13
7.5	18993.347	−2	18994.821	10
8.5	18993.240	−3	18994.900	10
9.5	18993.138	3	18994.971	8
10.5	18993.025	−1	18995.043	7
11.5	18992.911	−3	18995.120	11
12.5	18992.804	4	18995.183	6
13.5	18992.683	−3	18995.252	7
14.5	18992.574	4	18995.316	4
15.5	18992.452	1	18995.381	5
16.5	18992.334	3	18995.437	−1
17.5	18992.208	−2	18995.490	−9
18.5	18992.086	1	18995.549	−10
19.5	18991.951	−9		
20.5	18991.827	−6		
21.5	18991.698	−6		
22.5	18991.563	−10		
23.5	18991.431	−11		
24.5	18991.291	−16		
25.5	18991.165	−8		
26.5	18991.026	−9		
27.5	18990.891	−5		
28.5	18990.744	−10		
29.5	18990.609	−2		
30.5	18990.472	4		

small residuals, well below the experimental uncertainties (Tables 6 and 7). For C_6D the upper electronic state of the $\Omega = \frac{1}{2}$ component seems to be perturbed above $J' = 11.5$. Therefore, in the fit only lower levels have been included for the $\Omega = \frac{1}{2}$ component, resulting in a considerably smaller rms. The excited state molecular parameters are listed in Table 8. The rms of the fit for C_6H and C_6D are comparable (0.007 cm^{-1}) and well below the experimental linewidth (FWHM ≈ 0.035 cm^{-1}).

The rotational constant in the upper $^2\Pi$ electronic state for both C_6H and C_6D is 0.983% of the ground state value. This is close to the value found for the iso-electronic $C_6H_2^+$ triacetylene cation radical: 0.982% (*34*). It reflects the increase in overall length of the chain upon electronic excitation, which is calculated by deriving the center-of-mass coordinate of the hydrogen atom (z) using Kraitchman's equation (*35*). This yields an increase of z from 417.8 pm in the ground state to 418.6 pm in the electronically excited state.

TABLE 7
Measured Rotational Frequencies of the 0_0^0 $^2\Pi \leftarrow X^2\Pi$ Transition of C_6D

Transition J	ν (cm^{-1})	o–c ($10^{-3}cm^{-1}$)	ν (cm^{-1})	o–c ($10^{-3}cm^{-1}$)
$\Omega = 3/2$	P-branch		R-branch	
1.5			19037.007	0
2.5	19036.575	6	19037.096	5
3.5	19036.476	−2	19037.170	−3
4.5	19036.387	2	19037.245	−8
5.5	19036.291	0	19037.334	1
6.5	19036.197	2	19037.408	−3
7.5	19036.103	6	19037.486	−2
8.5	19035.999	0	19037.557	−6
9.5	19035.904	6	19037.632	−5
10.5	19035.802	4	19037.703	−6
11.5	19035.698	4	19037.774	−7
12.5	19035.592	2	19037.846	−4
13.5	19035.489	4	19037.920	2
14.5	19035.388	9	19038.981	−5
15.5	19035.277	7	19038.044	−7
16.5	19035.167	7		
17.5	19035.059	9		
18.5	19034.939	2		
19.5	19034.824	0		
20.5	19034.702	−7		
21.5	19034.581	−11		
22.5	19034.467	−8		
23.5	19034.356	1		
24.5	19034.233	−2		
25.5	19034.114	1		
26.5	19033.994	3		
27.5	19033.869	4		
28.5	19033.748	9		
29.5	19033.611	−2		
30.5	19033.482	−2		
31.5	19033.351	−4		
32.5	19033.216	−5		
$\Omega = 1/2$	P-branch		R-branch	
0.5			19045.861	−8
1.5	19045.592	−13	19045.955	0
2.5	19045.503	−11	19046.044	7
3.5	19045.413	−8	19046.112	−7
4.5	19045.326	−1	19046.189	−10
5.5	19045.233	2	19046.265	−12
6.5	19045.138	5	19046.355	0
7.5	19045.037	3	19046.424	−6
8.5	19044.939	6	19046.487	−16
9.5	19044.841	11	19046.574	−2
10.5	19044.741	15	19046.662	16
11.5	19044.633	12		
12.5	19044.530	17		

NOTE. The observed-calculated (o-c) are derived from the constants in Tables 5 and 8.

TABLE 8
Spectroscopic Constants (in cm^{-1}) for the Excited $^2\Pi$ State of C_6H and C_6D

Constant	C_6H	C_6D
A_{eff}	-23.6876(10)	-24.0755(14)
B'	0.0455976(17)	0.0435488(26)
D'	D''	D''
T_0	18989.7677(7)	19041.2653(8)

ACKNOWLEDGMENT

We are grateful to J. K. G. Watson and J. M. Brown for helpful discussions. This work has been supported by the Swiss National Science Foundation, project Number 20-55285.98, and NASA Grant NA95-4050.

REFERENCES

1. P. Thaddeus, M. C. McCarthy, M. J. Travers, C. A. Gottlieb, and W. Chen, *Faraday Discuss. Chem. Soc.* **109,** 121 (1998) [and references therein].
2. D. A. Kirkwood, H. Linnartz, M. Grutter, O. Dopfer, T. Motylewski, M. Pachkov, M. Tulej, M. Wyss, and J. P. Maier, *Faraday Discuss. Chem. Soc.* **109,** 109 (1998).
3. J. Cernicharo and M. Guélin, *Astron. Astrophys.* **309,** L27 (1996).
4. M. Guélin, J. Cernicharo, M. J. Travers, M. C. McCarthy, C. A. Gottlieb, P. Thaddeus, M. Ohishi, S. Saito, and S. Yamamoto, *Astron. Astrophys.* **317,** L1 (1997).
5. H. Suzuki, M. Ohishi, N. Kaifu, S. Ishikawa, and T. Kasuga, *Publ. Astron. Soc. Jpn* **38,** 911 (1986).
6. J. Cernicharo, M. Guélin, K. M. Menten, and C. M. Walmsley, *Astron. Astrophys.* **181,** L1 (1987).
7. M. Guélin, J. Cernicharo, C. Kahane, J. Gomez-Gonzalez, and C. M. Walmsley, *Astron. Astrophys.* **175,** L5 (1987).
8. S. Saito, K. Kawaguchi, H. Suzuki, M. Ohishi, N. Kaifu, and S. Ishikawa, *Publ. Astron. Soc. Jpn* **39,** 193 (1987).
9. P. F. Bernath, K. H. Hinkle, and J. J. Keady, *Science* **244,** 562 (1989).
10. J. P. Maier, *Chem. Soc. Rev.* **26,** 21 (1997).
11. J. P. Maier, *J. Phys. Chem. A* **102,** 3462 (1998).
12. C. A. Gottlieb, M. C. McCarthy, M. J. Travers, J.-U. Grabow, and P. Thaddeus, *J. Chem. Phys.* **109,** 5433 (1998).
13. M. C. McCarthy, J.-U. Grabow, M. J. Travers, W. Chen, C. A. Gottlieb, and P. Thaddeus, *Astrophys. J. Lett.* **494,** L231 (1998).
14. [See A. van Orden and R. J. Saykally, *Chem. Rev.* **98,** 2313 (1998) for references therein].
15. M. Ohara, H. Shiromaru, and Y. Achiba, *J. Chem. Phys.* **106,** 9992 (1997).
16. Y. Zhao, E. de Beer, C. Xu, T. Taylor, and D. M. Neumark, *J. Chem. Phys.* **105,** 4905 (1996).
17. M. Tulej, D. A. Kirkwood, G. Maccaferri, O. Dopfer, and J. P. Maier, *Chem. Phys.* **128,** 239 (1998).
18. K. Hoshina, H. Kohguchi, Y. Ohshima, and Y. Endo, *J. Chem. Phys.* **109,** 3465 (1998).
19. M. Kotterer and J. P. Maier, *Chem. Phys. Lett.* **266,** 342 (1997).
20. H. Linnartz, T. Motylewski, and J. P. Maier, *J. Chem. Phys.* **109,** 3819 (1998).
21. F. Pauzat and Y. Ellinger, *Astron. Astrophys.* **216,** 305 (1989).
22. O. V. Dorofeeva and L. V. Gurvich, *Thermochim. Acta* **197,** 53 (1992).
23. D. E. Woon, *Chem. Phys. Lett.* **244,** 45 (1995).
24. J. C. Pearson, C. A. Gottlieb, D. R. Woodward, and P. Thaddeus, *Astron. Astrophys.* **189,** L13 (1988).
25. M. C. McCarthy, M. J. Travers, A. Kovács, C. A. Gottlieb, and P. Thaddeus, *Astrophys. J. Suppl. Ser.* **113,** 105 (1998).
26. M. C. McCarthy, C. A. Gottlieb, A. L. Cooksy, and P. Thaddeus, *J. Chem. Phys.* **103,** 7779 (1995).
27. T. Motylewski and H. Linnartz, *Rev. Sci. Instrum.* **70,** 1305 (1999).
28. H. Linnartz, T. Motylewski, F. Maiwald, D. A. Roth, F. Lewen, I. Pak, and G. Winnewisser, *Chem. Phys. Lett.* **292,** 188 (1998).
29. J. M. Brown, E. A. Colbourn, J. K. G. Watson, and F. D. Wayne, *J. Mol. Spectrosc.* **74,** 294 (1979).
30. J. M. Brown, M. Kaise, C. M. L. Kerr, and D. J. Milton, *Mol. Phys.* **36,** 553 (1978).
31. M. C. McCarthy, W. Chen, A. J. Apponi, C. A. Gottlieb, and P. Thaddeus, *Astrophys. J.* **520,** 158 (1999).
32. C. H. Townes and A. L. Schawlow, "Microwave Spectroscopy," Dover, New York, 1955.
33. S. Yamamoto, S. Saito, H. Suzuki, S. Deguchi, N. Kaifu, S. Ishikawa, M. Ohishi, *Astrophys. J.* **348,** 363 (1990).
34. W. E. Sinclair, D. Pfluger, H. Linnartz, and J. P. Maier, *J. Chem. Phys.* **110,** 296 (1999).
35. J. Kraitchman, *Am. J. Phys.* **21,** 17 (1953).